Vol. 85, No. 21

The Latency-Associated UL138 Gene Product of Human Cytomegalovirus Sensitizes Cells to Tumor Necrosis Factor Alpha (TNF-α) Signaling by Upregulating TNF-α Receptor 1 Cell Surface Expression[▽]

Christina Montag,† Jutta Annabella Wagner,† Iris Gruska, Barbara Vetter,
Lüder Wiebusch, and Christian Hagemeier*

Children's Hospital, Laboratory for Molecular Biology, Charité Universitätsmedizin Berlin, Ziegelstr. 5-9, 10117 Berlin, Germany

Many viruses antagonize tumor necrosis factor alpha (TNF-α) signaling in order to counteract its antiviral properties. One way viruses achieve this goal is to reduce TNF-α receptor 1 (TNFR1) on the surface of infected cells. Such a mechanism is also employed by human cytomegalovirus (HCMV), as recently reported by others and us. On the other hand, TNF-α has also been shown to foster reactivation of HCMV from latency. By characterizing a new variant of HCMV AD169, we show here that TNFR1 downregulation by HCMV only becomes apparent upon infection of cells with HCMV strains lacking the so-called ULb′ region. This region contains genes involved in regulating viral immune escape, cell tropism, or latency and is typically lost from laboratory strains but present in low-passage strains and clinical isolates. We further show that although ULb′-positive viruses also contain the TNFR1-antagonizing function, this activity is masked by a dominant TNFR1 upregulation mediated by the ULb′ gene product UL138. Isolated expression of UL138 in the absence of viral infection upregulates TNFR1 surface expression and can rescue both TNFR1 reexpression and TNF-α responsiveness of cells infected with an HCMV mutant lacking the UL138-containing transcription unit. Given that the UL138 gene product is one of the few genes recognized to be expressed during HCMV latency and the known positive effects of TNF-α on viral reactivation, we suggest that via upregulating TNFR1 surface expression UL138 may sensitize latently infected cells to TNF-α-mediated reactivation of HCMV.

Human cytomegalovirus (HCMV) is a species-specific ubiquitous betaherpesvirus that has coevolved with humans and adapted its life cycle perfectly well to that of its host. Once primary infection has taken place the virus persists in individuals indefinitely by keeping a well-balanced presence between a latent state and triggered phases of reactivation that are supported by an optimized defense machinery against the host's immune system. Primary infection of healthy individuals with HCMV is normally asymptomatic, but in immunocompromised people infections can cause severe disease, and particularly in transplant recipients HCMV is a major health threat (24a).

HCMV is equipped with several genes that allow this virus to productively infect an unusually broad range of cells, including endothelial cells, epithelial cells, fibroblasts, and smooth muscle cells (40). During productive infection, viral gene expression occurs in a highly regulated manner, giving rise to a well-studied cascade of immediate-early (IE), early (E), and late (L) gene products (24a). In contrast, comparatively little is known about latently infected cells. *In vivo* and *in vitro* studies have identified few cell types that support latent infection. Typically, these were CD34$^+$ undifferentiated progenitor cells,

and reactivation and/or permissiveness usually goes hand in hand with their differentiation, which can, for instance, be triggered by cytokines like tumor necrosis factor alpha (TNF-α) (16, 19, 24, 26, 35, 41, 42, 46, 47). Similarly, in comparison to the virus' lytic cycle, there exists only a poor understanding of the genes that are required to induce, maintain, or exit the latent state of infection, and only few gene products have been identified at all whose expression is associated with latency. One, denominated LUNA, is derived as an antisense transcript from the UL81-82 locus (3). Another is an interleukin-10 homologue encoded by UL111.5A (22) and, finally, UL138 that is encoded in the ULb′ region (16). Of these, only the loss of UL138 has been demonstrated to compromise latent infection in an *in vitro* model system, whereas UL138 has been found to be dispensable for lytic infection (16).

Adaptation of HCMV to cell culture has long been recognized to cause several mutations to the coding capacity of the virus (34). One of the first differences noted was the loss of the so-called ULb′ region from extensively passaged laboratory strains, like Towne and AD169 (7, 8). In AD169-varATCC, the 19 ULb′ genes from the right end of the unique long (UL) segment have been replaced by an inverted duplication derived from the left end of the genome (RL), accompanied by a frameshift mutation in UL131A (7, 8, 11). Functionally, the entire ULb′ region is dispensable for lytic infection in fibroblasts but strictly required *in vivo* (48) and, in particular, the structural integrity of UL128-UL131A is a prerequisite for HCMV tropism for endothelial and epithelial cells *in vitro* (36). In addition, genes of the ULb′ region (UL146 and UL147)

have been implicated in immune modulation (37), immune evasion (UL141 and UL142) (49), NF-κB signaling (UL144) (33), and latency (UL138) (16, 31). Thus, the ULb′ region contributes important viral properties for HCMV infection *in vivo* but hampers infection of fibroblasts *in vitro*, resulting in a rapid selection against the responsible genes during propagation in these cells (10, 43).

Due to the antiviral properties of TNF-α and interferons, many viruses have evolved measures to counteract signaling pathways induced by these cytokines (2a, 20a). In the case of TNF-α, several viruses, including herpesviruses, specifically direct their countermeasures toward the major TNF-α receptor 1 (TNFR1). Epstein-Barr virus LMP-1 downregulates TNFR1 mRNA expression (9), whereas herpes simplex virus 1 contains an activity that actively degrades TNFR1 mRNA (25). Poliovirus protein 3A (30) and the adenovirus group C RID complex downregulate TNFR1 surface expression (13), and the papillomavirus 16 E6 protein and the poxvirus TNFR1 homologues directly bind to and inactivate TNFR1 (14, 38). Human cytomegalovirus has also been shown to antagonize TNF-α signaling (2, 21, 28) by downregulating TNFR1 surface expression (2, 28). Thus, targeting TNFR1 is a common principle during virus infection, and this normally antagonizes TNF-α signaling.

Here, we show that ULb′-encoded UL138 upregulates TNFR1 surface expression during HCMV infection, thereby sensitizing infected cells to TNF-α signaling. Given the expression of UL138 during latent HCMV infection and the positive effect of TNF-α on HCMV reactivation, our results suggest that UL138 may foster reactivation of the lytic HCMV cycle by sensitizing latently infected cells to TNF-α via increasing TNFR1 availability on the host cell surface.

MATERIALS AND METHODS

Cells. Human embryonic lung (HEL) fibroblasts (Fi301; obtained from the Institute of Virology, Charité, Berlin, Germany) were maintained in Eagle's minimum essential medium (EMEM) from Lonza (Walkersville, MD) supplemented with 1 mM sodium pyruvate, 2 mM L-alanyl-L-glutamine, nonessential amino acids, 0.75% (wt/vol) sodium bicarbonate, 50 μg/ml gentamicin, and 10% fetal bovine serum (FBS). HeLa cells (ATCC, Manassas, VA) were maintained in Dulbecco's modified Eagle medium (DMEM) supplemented with 10% FBS, 2 mM L-alanyl-L-glutamine, 100 U/ml penicillin, and 100 μg/ml streptomycin. Cells were passaged 1:3 every 3 days. THP-1 suspension cells (Institute of Cardiology, Charité, Berlin, Germany) were maintained in RPMI 1640 medium (Invitrogen, Carlsbad, CA) supplemented with 10% FBS, 0.05 mM 2-mercaptoethanol, 100 U/ml penicillin, and 100 μg/ml streptomycin. Fresh medium was added when the cell density reached 8×10^5 viable cells/ml.

Viruses. HCMV strains AD169 and Davis were purchased from ATCC (Manassas, VA). Merlin and Toledo strains were a gift from Gavin Wilkinson (Cardiff, United Kingdom). Strain AD169-varT was a gift from Bodo Plachter (Mainz, Germany), and strain Towne was kindly provided by Richard Greaves (Cambridge, United Kingdom) (18). By PCR analysis this strain was found to resemble Towne_short. The AD169-BAC and Toledo-BAC strains were kindly provided by Gaby Hahn (Ingolstadt, Germany), and the ToldeoΔ15kb-BAC was a generous gift from Hua Zhu (Newark, NJ). All strains were grown on HEL fibroblasts. Virus titers were determined by IE1/IE2 fluorescence as described previously (51). Briefly, quiescent HEL fibroblasts were infected with various dilutions of virus stocks. After 24 h of incubation, cells were fixed in 75% ethanol and stained with an IE1/IE2-specific antibody. The number of positive cells was determined by flow cytometry and used to calculate viral titers.

Virus infection and NF-κB activation. For infection, HEL fibroblasts at 75% confluence were serum starved for 3 days and infected with different HCMV strains at a multiplicity of infection (MOI) of 5 in the presence of serum supplemented with 10% FCS. For coinfection experiments, cells were infected with an MOI of 2.5. Virus adsorption was allowed for 1 h, and mock-infected control

cultures were exposed to an equal volume of medium containing the same serum concentration. HCMV-dependent regulation of NF-κB activity was determined at 72 h postinfection (hpi) by stimulation with 5 ng/ml TNF-α (Sigma-Aldrich, St. Louis, MO) for 10 min (electrophoretic mobility shift assay [EMSA] and immunoblotting) or 120 min (real time-PCR). Phosporylation of the NF-κB inhibitor IκBα was detected in the presence of 100 μg/ml acetyl-L-leucyl-[SCAP]L-leucyl-L-norleucinal (ALLN; Sigma-Aldrich, St. Louis, MO), a proteasome inhibitor that prevents the rapid turnover of phosphorylated IκBα. ALLN was added 1 h prior to TNF-α stimulation (0.01 ng/ml; 10 min).

Antibodies. IκBα (C15), pp28 (CH19), c-myc (9E10), vigilin (2404C3a), and glyceraldehyde-3-phosphate dehydrogenase (GAPDH; 6C5) antibodies were purchased from Santa Cruz Biotechnolgoy (Santa Cruz, CA). The gB antibody was purchased from Abi (Frankfurt, Germany), and the IE1/IE2 (E13) antibody was received from Argene (Varilhes, France). For fluorescence-activated cell sorting analysis, a TNFR1 antibody (MAB225) from R&D systems (Minneapolis, MN), a bromodeoxyuridine (BrdU) antibody (555627) from BD Biosciences (San Jose, CA), and Alexa Fluor 647 and Alexa Fluor 488 mouse IgG1 secondary antibodies from Invitrogen (Carlsbad, CA) were used.

BAC mutagenesis. Homologous recombination was used to generate the Toledo knockout mutants. Genes of interest were replaced by a kanamycin resistance cassette from the plasmid pSLFRTKn (1), kindly provided by Wolfram Brune (Hamburg, Germany). DNA fragments were generated by PCR (primer sequences are provided in Table 1), using pSLFRTKn as template. PCR products were digested with DpnI, purified, and electroporated into *Escherichia coli* DH10B containing the Toledo-WT-BAC and the pKD46 plasmid carrying the exo, bet, and gam recombination enzymes under an arabinose-inducible promoter kindly provided by Gabi Hahn (Ingolstadt, Germany). Cells were grown in the presence of chloramphenicol (bacterial artificial chromosome [BAC]) and ampicillin (pKD46) at 30°C, and recombination was induced by addition of arabinose (0.1%, wt/vol). Positive clones were identified by PCR analysis. DNA was prepared using Macherey and Nagel columns and transfected into HEL fibroblasts. Cells were passaged 1:3 every 3 days until viral plaques could be detected. Virus-containing supernatants were harvested, and virus titers were determined as described above.

Lentiviral transduction. The lentiviral expression vector pCDH-CMV-MCS-EF1-GreenPuro from SBI (Mountain View, CA) was used to express HCMV Toledo UL133, UL135, UL136, and UL138 open reading frames (ORFs) with a C-terminal in-frame Myc tag (primer sequences are shown in Table 2). To produce lentiviral stocks, the expression plasmids were cotransfected with the lentiviral packaging plasmids psPAX2 and pMD2G into proliferating HEK293T cells with Lipofectamine 2000 (Invitrogen, Carlsbad, CA). At 48 h posttransfection, virus-containing cell culture supernatants were harvested and deep frozen in aliquots. An MOI of 1 was used for the lentiviral transduction of fibroblasts. Between 2 to 4 days after infection, puromycin (4 μg/ml) was added to the culture medium to eliminate remaining uninfected cells.

Transfections. Lentiviral expression plasmids were transfected into HeLa cells with TurboFect (Fermentas, St. Leon-Rot, Germany) according to the manufacturer's instructions. For generation of mutant HCMV viruses, BAC-DNA, pcDNA-pp71 flag (Bodo Plachter, Mainz, Germany), and pBRep-Cre (Wolfram Brune, Hamburg, Germany) were cotransfected into HEL fibroblasts by using ExGen 500 (Fermentas, St. Leon-Rot, Germany) as the transfection reagent. Medium was changed 24 h posttransfection, and transfected cells were split 1:3 every 3 days until plaques could be detected.

Nucleotransfection. Nucleotransfections were performed using the basic nucleofector kit for primary mammalian fibroblasts (Lonza, Walkersville, MD) and an Amaxa Nucleofector (Lonza, Basel, Switzerland) according to the manufacturer's instructions with minor modifications. Briefly, confluent HEL fibroblasts either transduced with a UL138-expressing lentivirus or a lentiviral control vector were cultured in EMEM supplemented with 0.5% FCS. After 72 h, serum-starved cells were trypsinized, and 1×10^6 cells together with 4 μg DNA and 100 μl nucleofector solution were electroporated into HEL fibroblasts by applying the A-023 nucleofector program. Cells were electroporated with a pcDNA3 control vector or a submajor immediate-early (sub-MIE) construct containing a subgenomic fragment of HCMV covering nucleotides −1338 to +8409 relative to the transcription start site of the MIE gene promoter (51a). After nucleofection, cells were transferred into 4 ml preequilibrated EMEM without FCS and distributed equally to 2 wells of a 6-well plate. One aliquot was directly stimulated with TNF-α (30 ng/ml) for 4 h, and one was left unstimulated. After 4 h cells were harvested, RNA was prepared, and IE gene expression was measured by real-time PCR.

Gene expression array. Total RNA from AD169-varATCC- and AD169-varT-infected HEL fibroblasts was prepared with TRIzol reagent (Invitrogen, Carlsbad, CA) according to the manufacturer's instructions. The cDNA microarray

TABLE 1. Primers used for BAC recombineering

Knockout primer	Sequence
ToledoΔUL133-138 fw	5′-ATGGGTTGCGACGTGCACGATCCTTCGTGGCAATGCCAATGGGGCGTTCCCGTCGTGGAATGCCTTCGAATTC-3′
ToledoΔUL133-138 rv	5′-GTCAAAGCGACATTATCGCGATCCGCTCCCCTCTTTTTTCTTTTTCTCATACAAGGACGACGACGACAAGTAA-3′
ToledoΔUL139-144 fw	5′-GCTGATTGTTACGACAAACGAGTTGGTATATCCATTATATAGTAACGAACCGTCGTGGAATGCCTTCGAATTC-3′
ToledoΔUL139-144 rv	5′-TTATCTGTGTGACTTCATCGTACCGTGATGTAAAAACAACAACAGGAAGCACAAGGACGACGACGACAAGTAA-3′
ToledoΔUL145-148 fw	5′-TGCAGCTTGGAGTGACTAAAGTGTGTCAGCATAATGAAGTGCAACTGGGCCGTCGTGGAATGCCTTCGAATTC-3′
ToledoΔUL145-148 rv	5′-ATCGCCGCCATCATTGTAATCAGCAATGTGTTGAGGTACTGCACGATGAAACAAGGACGACGACGACAAGTAA-3′
ToledoΔUL148A-D fw	5′-TTGTACCCCCCTTCCCCTCCGTGTTGTAGCCCATCGGCCGCGGCGATCTCCGTCGTGGAATGCCTTCGAATTC-3′
ToledoΔUL148A-D rv	5′-TTTTCCTGTGTTAACACCGGCGTTTTTGGGACGGTCGGTTAACGTGGGTTACAAGGACGACGACGACAAGTAA-3′
ToledoΔUL149-151 fw	5′-CAGTGTTGCTATCGTCATCTTCATCGGAGTCTGTCTGGTGGCCCTGATGTCGTCGTGGAATGCCTTCGAATTC-3′
ToledoΔUL149-151 rv	5′-CATGGTCTTTGTCAGCGGCACGGCGCTGGGGACGGGGTTTCACCGCGCTGACAAGGACGACGACGACAAGTAA-3′

was performed at the Center for Applied Genomics (Newark, NJ) according to the methods described by Yang et al. (50).

Immunoblotting. The preparation of cell lysates and immunoblotting experiments have been described previously (28).

EMSAs. The preparation of nuclear extracts and EMSA experiments have been described previously (28).

Real time-PCR. Total RNA was prepared with TRIzol reagent (Invitrogen, Carlsbad, CA) according to the manufacturer's instructions and quantified by UV-spectrophotometry. For quantitative real-time PCR analysis, cDNA was synthesized from total RNA by using the QuantiTect reverse transcription kit (Qiagen, Hilden, Germany). The equivalent of 5 ng of RNA was used as input for each PCR (primer sequences are provided in Table 3). PCRs were performed in a total volume of 10 μl, using the Power SYBR green PCR master mix (Applied Biosystems, Foster City, CA), following the manufacturer's instructions. Real time-PCR was performed on an ABI 7500 Fast real-time PCR system (Applied Biosystems, Foster City, CA) with a standard amplification protocol: 95°C for 10 min, followed by 40 cycles of 95°C for 15 s and 60°C for 1 min. Each analysis was performed in triplicate. Relative Traf-1 or IE mRNA expression levels were calculated and normalized to GAPDH or L32 expression levels by using ABI 7500 software (version 2.0.1; Applied Biosystems, Foster City, CA).

Flow cytometry. Cells were harvested by trypsinization, and 10^5 cells were incubated in 25 μl phosphate-buffered saline (PBS) containing 0.5% bovine serum albumin and 2 ng/μl of either a TNFR1 antibody or a BrdU antibody as isotype control for 30 min at 4°C. Cells were washed once in PBS and incubated with an Alexa Fluor 647-conjugated secondary antibody for another 30 min at 4°C in the dark. Viral kinetic classes were determined by staining of ethanol-fixed HEL fibroblasts with IE1/IE1, gB, and pp28 antibodies as previously described (51). Cells were washed once with PBS and incubated with a secondary Alexa Fluor 488 mouse antibody. Cells were washed twice with PBS and analyzed with a FACSCanto2 flow cytometer (BD Biosciences, San Jose, CA) using the FlowJo software (version 7.2.4.; Tree Star Inc., Ashland, OR). Statistical calculations were also performed with the FlowJo software package.

RESULTS

Our recent work had identified a previously uncharacterized AD169 variant on the basis of its inability to counteract TNF-α-induced NF-κB activation (28). By employing a comparative restriction length analysis using genomic DNAs of a number of well-characterized viral strains (including AD169, Towne, Davis, and Merlin) and several restriction enzymes (ClaI, HpaI, SpeI, and EcoRI), we were able to show that this virus is structurally most related to AD169-varATCC (28) (data not shown). Hence, this virus was denominated by us as AD169-varT, referring to both its structural relatedness and a characteristic functional feature. Thus, AD169-varT and AD169-varATCC are closely related, and the functional differences that initially led to the identification of AD169-varT are paralleled by tractable structural differences.

AD169-varT contains additional genetic information and acts dominantly over AD169-varATCC in TNF-α responsiveness. In order to identify the viral gene product(s) responsible for the observed functional differences, we followed up on the hypothesis that they may be linked to the demonstrated structural differences. In principle, the functional differences could be due to either a loss or gain of complete (sets of) genes or more subtle differences, like DNA sequence variations within confined genes. Given the observation from the restriction length analyses, we favored the possibility of gains or losses of

TABLE 2. Primers used for cloning of lentiviral expression plasmids

Primer name	Sequence
Tol ORF 133-XbaI-fw	5′-CGCTCTAGAATGGGTTGCGACGTGCACGA-3′
Tol ORF 133-BamHI-myc-rv	5′-CCGGATCCCTACAGATCTTCTTCAGAAATAAGTTTTT GTTCCGTTCCGGTCTGATGCTGC-3′
Tol ORF 135-XbaI-fw	5′-CGCTCTAGAATGTCCGTACACCGGCCCTTC-3′
Tol ORF 135-BamHI-myc-r	5′-CCGGATCCCTACAGATCTTCTTCAGAAATAAGTTTTT GTTCGGTCATCTGCATCGACTCG-3′
Tol ORF 136-XbaI-fw	5′-CGCTCTAGAATGTCAGTCAAGGGCGTGGA-3′
Tol ORF 136-BamHI-myc-rv	5′-CCGGATCCCTACAGATCTTCTTCAGAAATAAGTTTTT GTTCCGTAGCGGGAGATACGG-3′
Tol ORF 138-XbaI-fw	5′-CGCTCTAGAATGGACGATCTGCCGCTGAA-3′
Tol ORF 138-EcoRI-myc-rv	5′-CGAATTCCTACAGATCTTCTTCAGAAATAAGTTTTT GTTCCGTGTACTCTTGATG-3′

Primer name	Sequence
Traf1 real time-fw	5′-GCCCTTCCGGAACAAGGTC-3′
Traf1 real time-rv	5′-CGTCAATGGCGTGCTCAC-3′
GAPDH real time-fw	5′-TTCACCACCATGGAGAAGG-3′
GAPDH real time-rv	5′-CACACCCATCACAAACATGG-3′
IEexon3 real time-fw	5′-TCTGCCAGGACATCTTTCTCG−3′
IEexon3 real time-rv	5′-GGAGACCCGCTGTTTCCAG−3′
L32 real time-fw	5′-CAAGGAGCTGGAAGTGCT-3′
L32 real time-rv	5′-CAGCTCTTTCCACGATGG-3′

complete genes. To systematically address this point, we made use of a commercially available gene expression array of the HCMV genome that covers the 194 open reading frames of AD169-varATCC and 19 additional open reading frames found in the Toledo strain. The complete list of represented genes can be found at http://www.cag.icph.org/microarray .html. This HCMV gene array has recently been used to demonstrate gene expression differences between strains AD169 and Toledo (50).

Primary fibroblasts were infected either with plaque-purified AD169-varATCC or AD169-varT. At 72 hpi cells were harvested and total RNAs were prepared. An aliquot of cells was used to control for the inhibitory effect of the two AD169 variants on TNF-α-induced NF-κB activation (data not shown). Cy3-labeled (AD169-varATCC) or Cy5-labeled (AD169-varT) probes were hybridized to the array in triplicates, and dye swap experiments were performed to account for hybridization artifacts due to labeling differences. Thus, genes equally expressed in both infected cultures should result in an expression ratio of 1, and deviance from 1 indicates under- or overrepresented transcripts in one of the infected cultures.

The results of the screen were surprisingly clear-cut and are shown in Fig. 1. All differences in mRNA abundance of viral genes were defined to two genomic regions of HCMV. First, genes representing the internal repeat long (IRL) region (IRL1 to -14) were underrepresented in the AD169-varT-infected cells. However, transcripts of these genes were clearly detectable over background, and the degree of overexpression in AD169-varATCC-infected cells varied over a small range between 1.54- and 3.56-fold. Second, transcripts representing ULb′ genes that were not detectable over background in AD169-varATCC-infected cells were clearly present in cells infected with AD169-varT. Here, the range of expression differences varied from 2.03- to 49.91-fold over background, indicating that ULb′ genes are represented in AD169-varT and expressed with different intensities. The two most prominently expressed transcripts from this region derive from UL136 and UL138 (Fig. 1A).

This result was rather unexpected, since the genomes of high-passage laboratory strains characteristically contain a deletion of the ULb′ region that in turn has been replaced by an inverted duplication of a region from the left end of the genome, i.e., the IRL (7). Consistent with the gain of ULb′ gene transcripts found in AD169-varT-infected cells, transcripts from IRL genes are roughly halved compared to AD169-varATCC-infected cells, indicating that the IRL region has not been duplicated in AD169-varT.

While this work was in progress, Bradley et al. published an unusual AD169 variant (AD169-varUC) that also contained the ULb′ gene region (5). However, AD169-varUC also contains a characteristic internal deletion of 3.2 kb in its ULb′ region covering UL141 to UL143 and, at its 5′ and 3′ ends, respectively, parts of UL140 and UL144 (GenBank accession number FJ527563.1) (Fig. 1B). Amplification across this genomic section of AD169-varT employing primers upstream of UL140 and downstream of UL145 demonstrated that AD169-varT contains a corresponding deletion of just over 3 kb (Fig. 1C). DNA sequencing of this amplicon revealed that AD169-varT is indeed identical to AD169-varUC in this region (data not shown). Therefore, this analysis strongly suggested that AD169-varT and AD169-varUC represent the same HCMV strain, which deviated from the original clinical isolate prior to the loss of the ULb′ gene region as originally suggested by Bradley et al. (5).

The above data show that AD169-varT, which cannot counteract TNF-α-mediated NF-κB activity (28), contains an additional genomic region compared to AD169-varATCC, which in turn is a strong inhibitor of TNF-α-induced NF-κB activation. If this apparent lack of a TNF-α-antagonizing activity were causally linked to the additional genetic information found in AD169-varT, we wondered whether this virus acts dominantly over AD169-varATCC in coinfections. Therefore, we performed a set of experiments where the two AD169 variants were used to infect primary fibroblasts in the presence of TNF-α, either alone or in combination. As expected and previously shown, AD169-varATCC strongly counteracted TNF-α-induced NF-κB activation, whereas AD169-varT failed to do so (Fig. 2, lanes 1 to 8). However, when cells where simultaneously infected with both variants, TNF-α-induced NF-κB activation was strong (lanes 9 to 11), showing that indeed varT can act dominantly over varATCC. This finding suggested that varT delivers to AD169-varATCC-infected cells additional genetic information that is not present in AD169-varATCC and that encodes a counteracting activity of the AD169-varATCC-mediated inhibition of TNF-α-induced NF-κB stimulation. Thus, AD169-varATCC rather than AD169-varT appears to be a loss-of-function mutant that can only antagonize TNF-α-induced NF-κB activation, whereas AD169-varT can somehow counteract this inhibitory activity. The net effect of this apparent double negative regulatory circuit is the maintenance of the TNF-α signaling pathway in ULb′-positive, i.e., wild-type-resembling, HCMV-infected cells.

The ULb′ region regulates TNF-α responsiveness of infected cells. The above results suggested but did not prove that TNF-α-induced NF-κB activation is regulated by one or more genes from the ULb′ region. In order to address this point more directly, we first used different HCMV strains that either contain (AD169-varT, Toledo, Merlin, and Davis) or lack (AD169-varATCC and Towne) the ULb′ region and asked how these viruses would regulate TNF-α-induced NF-κB activation. Figure 3A shows that all viruses containing the ULb′ gene region maintained TNF-α-induced NF-κB activation during infection, whereas the two viral strains lacking the ULb′ region downregulated NF-κB activity.

To directly test whether the presence of the ULb′ region was responsible for the observed effects, we made use of the Toledo strain and a mutant derived thereof that lacked a 15-kb fragment encompassing the ULb′ region (Fig. 3B) (48). When
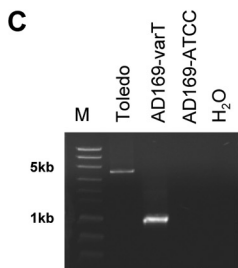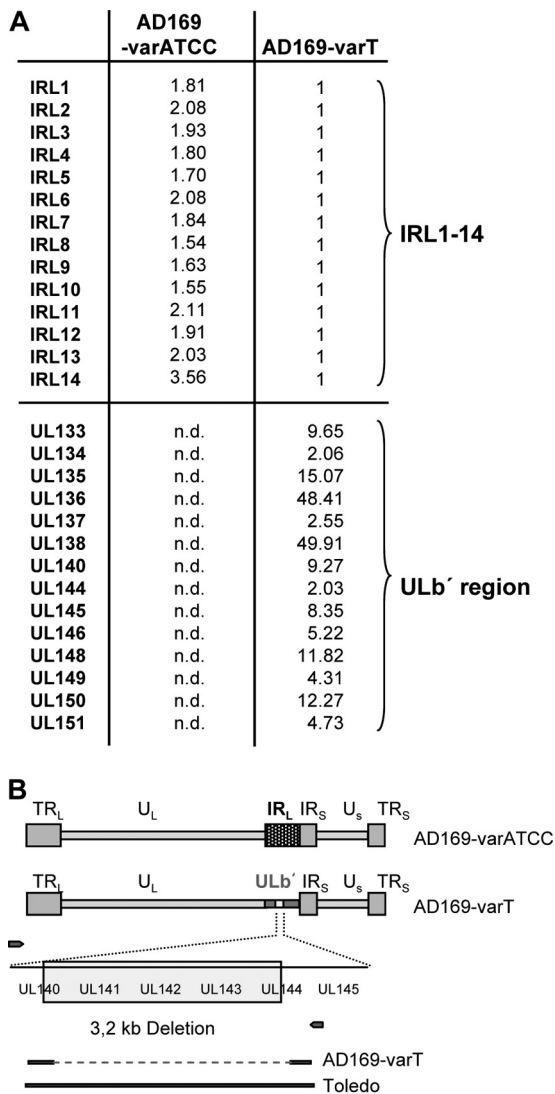
A

	AD169 -varATCC	AD169-varT	
IRL1	1.81	1	
IRL2	2.08	1	
IRL3	1.93	1	
IRL4	1.80	1	
IRL5	1.70	1	
IRL6	2.08	1	IRL1-14
IRL7	1.84	1	
IRL8	1.54	1	
IRL9	1.63	1	
IRL10	1.55	1	
IRL11	2.11	1	
IRL12	1.91	1	
IRL13	2.03	1	
IRL14	3.56	1	
UL133	n.d.	9.65	
UL134	n.d.	2.06	
UL135	n.d.	15.07	
UL136	n.d.	48.41	
UL137	n.d.	2.55	
UL138	n.d.	49.91	
UL140	n.d.	9.27	
UL144	n.d.	2.03	ULb′ region
UL145	n.d.	8.35	
UL146	n.d.	5.22	
UL148	n.d.	11.82	
UL149	n.d.	4.31	
UL150	n.d.	12.27	
UL151	n.d.	4.73	

B

C

FIG. 1. AD169-varT contains ULb′ region genes. (A) RNAs from cells infected with either AD169-varATCC or AD169-varT for 72 h were compared by microarray analysis. Only genes found to be differentially expressed are listed. Expression of IRL11-4 gene family members in AD169-varT-infected cells was set to a relative intensity of 1. Expression levels of IRL1-14 genes from AD169-varATCC-infected cells is shown as the fold increase. Transcripts of the listed ULb′ genes were not detected (n.d.) over background in AD169-varATCC-infected cells. Expression levels of these genes in AD169-varT-infected cells is shown as the fold increase over background measurements. Thus, scores for genes either equally expressed or lacking in both variants were approximately 1, and for matters of clarity those were omitted from the illustration. As detailed in panels B and C, genes for UL141 to -143 genes were lacking from the ULb′ region of AD169varT and are therefore not listed. (B) Schematics of the genomic architec-

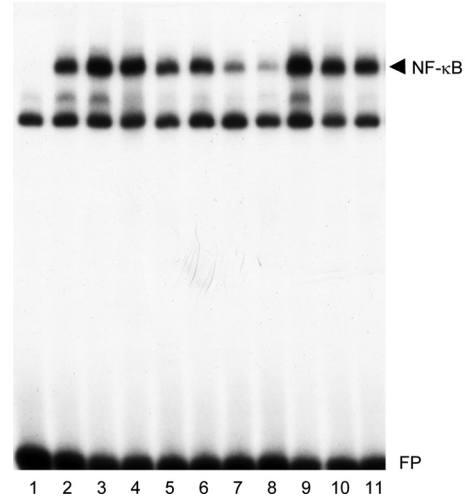

FIG. 2. Coinfection of AD169-varT prevents AD169-varATCC-mediated inhibition of TNF-α-induced NF-κB activation. HEL fibroblasts were infected for the indicated periods of time with either AD169-varATCC or AD169-varT (at an MOI of 5) or both (at an MOI of 2.5 each). After treatment of cells with 5 ng/μl TNF-α for 10 min, cells were harvested and nuclear extracts prepared. NF-κB DNA binding (black arrow) was detected by EMSA using a radioactive probe containing the NF-κB site of the major histocompatibility complex class I promoter.

analyzed side by side with the two AD169 variants, the ToledoΔ15kB mutant behaved like AD169-varATCC, i.e., it suppressed TNF-α-induced NF-κB activation, whereas wild-type Toledo was able to maintain activated NF-κB after TNF-α stimulation and, therefore, showed an AD169-varT-like phenotype (Fig. 3C, upper panel). Consistent with the NF-κB DNA binding profile, TNF-α-induced IκBα degradation was inhibited only in AD169-varATCC and ToledoΔ15kb-infected cells (Fig. 3C, lower panel), supporting a previous conclusion that HCMV affects the TNF-α influence on NF-κB signaling at an upstream level of the pathway. Thus, the ability to counteract TNF-α-induced NF-κB activity is indeed linked to the absence of the ULb′ region, suggesting that this genomic fragment contains one or more genes that act as a functional agonist of TNF-α signaling.

HCMV has been shown to regulate cell surface expression of TNFR1 (2) and, furthermore, TNFR1 regulation correlates with the sensitivity of HCMV-infected cells to TNF-α treat-

tures of AD169-varATCC and AD169-varT as delineated from the microarray analysis. The blow-up shows a subfragment of the ULb′ region present in AD169-varUC, containing a characteristic deletion encompassing 3′ sequences of UL140, the entire UL141, UL142, and UL143 genes, as well as 5′ sequences of UL144 (5). Small arrows to the left and right of the deleted region reflect the position of a primer pair that was used to amplify this region from AD169-varT. Bold and dotted lines shown below are the relative expected sizes of the amplification products when using this primer pair on strains Toledo and AD169-varT, respectively. (C) PCR products of the amplification using the depicted primer pair.
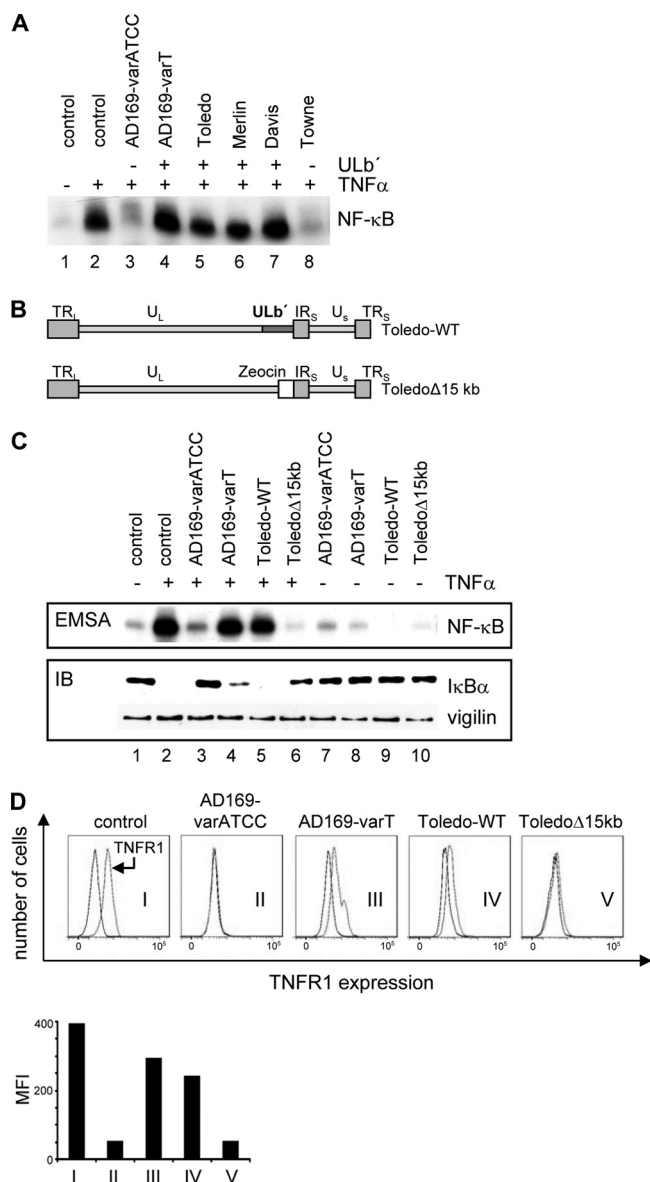
FIG. 3. The ULb′ region prevents inhibition of TNF-α-induced NF-κB activation. (A) Cells were infected for 72 h with different HCMV strains either known to contain (+) or to lack (−) ULb′ genes, followed by a 10-min treatment with TNF-α. NF-κB DNA binding was analyzed by EMSA. (B) Schematic showing the genomic architecture of the wild-type strain Toledo and mutant thereof lacking the ULb′ region (ToledoΔ15kb). The two strains were kindly provided by Hua Zhu (48). (C) HEL fibroblasts were infected with the different viral strains, variants, and mutants for 72 h as indicated, and cells were either treated with TNF-α (lanes 2 and 3 to 6) or left untreated (lanes 1 and 7 to 10). Nuclear extracts were prepared, and NF-κB DNA binding was analyzed by EMSA (upper panel). Protein extracts from the same cell populations were used to analyze IκBα abundance by immunoblotting (IB; lower panel). An antibody against vigilin was used to control for equal protein loading. (D) To analyze surface expression of TNFR1, control cells and cells infected with HCMV, as indicated, were harvested 72 hpi and incubated with either TNFR1-specific or isotype control antibodies. Surface expression of TNFR1 was analyzed by flow cytometry, and histograms were generated with the FlowJo analysis software (Becton Dickinson). Results are expressed as the mean fluorescence intensity (MFI) minus that of an isotype-matched antibody.

ment (28). To address whether TNFR1 surface expression may be regulated by ULb′ genes, we next determined TNFR1 expression on infected fibroblasts. Figure 3D shows that, like AD169-varATCC, ToledoΔ15kb led to a pronounced down-regulation of TNFR1 on the surface of infected cells (graphs II and V). However, the ULb′ region of Toledo, like AD169-varT, appears to counteract this effect to a significant degree (graphs III and IV). Of note, TNFR1 surface expression was analyzed in the absence of TNF-α treatment, suggesting that it is a consequence of the infection *per se* and not a mere internalization after ligand binding. Thus, ULb′ genes regulate TNF-α sensitivity during HCMV infection and maintain TNFR1 surface expression. These observations are most consistent with the view that the ULb′ region regulates TNF-α responsiveness by securing the availability of TNFR1 on HCMV-infected cells.

UL138 upregulates TNFR1 surface expression, sensitizing HCMV-infected cells to TNF-α-mediated NF-κB activation. We next designed five mutants within the Toledo background that were lacking distinct sets of genes from the ULb′ region, as indicated in Fig. 4A, in order to narrow the number of genes responsible for TNF-α responsiveness. In so doing, all genes described for this region were deleted in one of the mutants, with the exception of UL130-UL132. In AD169-varATCC (GenBank accession number NC_001347), these genes are still present at the left-hand border of the internal repeat and, therefore, should not serve as candidate genes for the observed activity.

All mutants resulted in comparable titers of progeny virus, which were then tested side by side for their ability to regulate both NF-κB DNA binding after TNF-α stimulation and TNFR1 surface expression. Only the mutant lacking the UL133 to -138 genes had lost the ability to maintain high NF-κB DNA binding activity in infected cells, and all other deletion mutants behaved like the Toledo wild type, i.e., they did not counteract NF-κB DNA binding (Fig. 4B). Although with the ΔUL133-138 mutant we did not observe the full degree of NF-κB-antagonizing activity as with ToledoΔ15kb, we always observed a consistently strong effect. However, TolΔUL133-138 still allowed residual NF-κB DNA binding, suggesting a UL133-UL138-independent additional activity encoded in the ULb′ region that can regulate TNF-α-mediated NF-κB DNA binding. This notion was also reflected by the quantitative analysis of three independent experiments, in which NF-κB DNA binding activity was determined by phosphorimaging (Fig. 4C). Since none of the mutants activated NF-κB DNA binding activity in the absence of TNF-α to an appreciable extent at 48 hpi, we concluded from this analysis that the UL133-138 gene region is necessary to maintain NF-κB DNA binding activity after TNF-α stimulation of HCMV-infected cells. Consistent with this observation, ToledoΔUL133-138, like the Δ15kb mutant, failed to maintain the degree of TNFR1 surface expression seen in cells infected with Toledo wild type (Fig. 4D). Importantly, the observed differences between Toledo wild type and the ΔUL133-138 mutant were not a consequence of differences in their respective infectious cycles, as judged by their virtually identical expression kinetics of IE, E, and L genes (Fig. 5). Thus, the UL133-138 region is responsible both for a sustained TNFR1 surface expression in HCMV-infected cells and NF-κB DNA
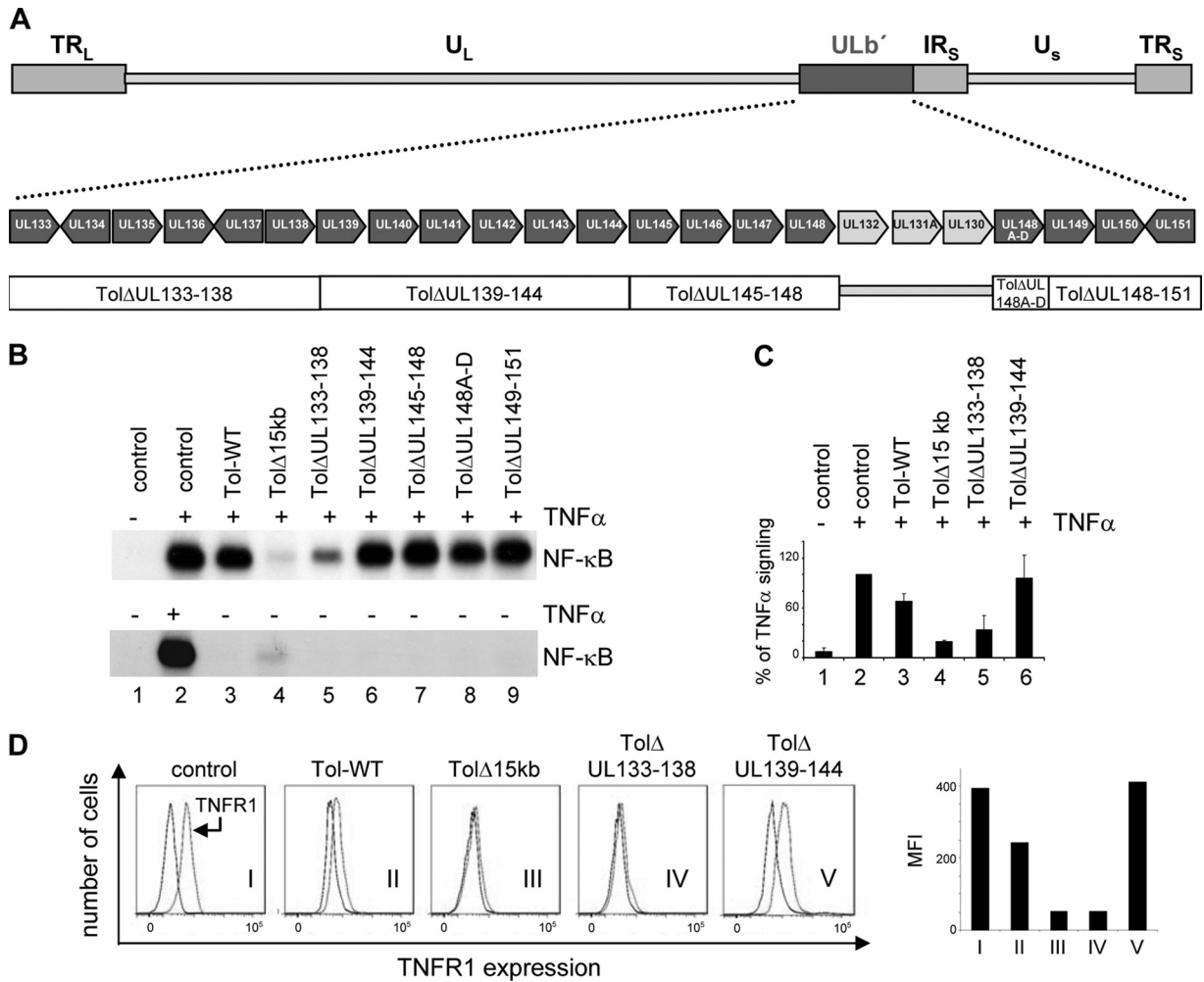
FIG. 4. Deletion of the UL133 to UL138 genes is sufficient to reinstall the inhibition of TNF-α-induced NF-κB activation by HCMV. (A) Schematic illustration of Toledo knockout mutants within the ULb′ region. UL133 to UL151 genes were grouped and deleted in 5 sets from the Toledo BAC as indicated. UL130 to UL132 were not included, since these genes are present in both AD169-varATCC and AD169-varT and should therefore not account for the functional differences of these strains. (B) Primary fibroblasts were infected with Toledo knockout mutants as indicated for 72 h and either treated (+) or not treated (−) with TNF-α. NF-κB DNA binding was detected by EMSA. (C) Quantitative analysis of three independent EMSA experiments by phosphorimaging. (D) Surface expression of TNFR1 on control cells and cells infected with HCMV as indicated was performed as described for Fig. 3D.

binding activity after TNF-α stimulation, suggesting that this gene region maintains TNF-α signaling to NF-κB by securing sufficient availability of TNFR1 at the surface of HCMV-infected cells.

The UL133 to -138 genes are transcribed in a polycistronic manner, i.e., all translation products arise from a single transcript (17, 31). This particularity made a further mutational analysis on the basis of open reading frame-specific deletions prone to unwanted effects from the expression of neighboring gene products, which would be difficult to control for in the absence of available antibodies to the encoded protein products. To circumvent this potential problem, we changed our strategy and decided to express each of the gene products from this region separately to determine whether any of them would be sufficient to regulate TNFR1 signaling in the absence of an HCMV infection. To this end we cloned cDNAs of UL133, UL135, UL136, and UL138 in frame with an epitope tag de-

rived from the c-myc gene into a lentiviral expression vector that also contained a green fluorescent protein (GFP) expression cassette. Transfection of HeLa cells followed by immunoblot analysis demonstrated that all proteins were stably produced in the absence of an HCMV infection, albeit with some degree of difference in expression levels (Fig. 6A). GFP-positive cells of transfected populations where then gated, and TNFR1 surface expression was determined. Clearly, UL138 but none of the other gene products was able to upregulate TNFR1 surface expression in HeLa cells (Fig. 6B). Similarly, UL134 was not able to upregulate TNFR1 surface expression (data not shown). As shown in Fig. 6C, this TNFR1 upregulation was functionally significant, since UL138 sensitizes the expression of a typical endogenous NF-κB target gene (Traf1) to limiting amounts of TNF-α. Also, UL138 alone can induce upstream events in the NF-κB signaling pathway, as shown by the TNF-α-dependent appearance of the phosphorylated and
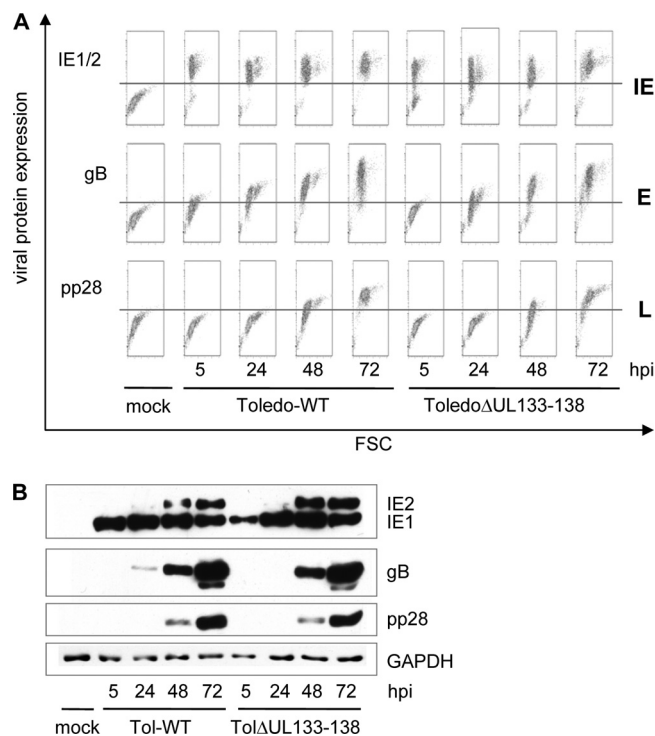
FIG. 5. Toledo wild-type (WT) and ToledoΔUL133-138 express IE, E, and L genes with similar kinetics. Primary fibroblasts were infected with Toledo WT or ToledoΔUL133-138 as indicated. (A) Cells were harvested at the indicated time points, fixed in ethanol, and stained with IE1/IE2 antibodies to detect IE gene expression, an anti-gB antibody to assess expression of a representative of early gene expression, and an antibody directed against pp28 to analyze late gene expression. Alexa Fluor 488 fluorescence was measured by flow cytometry. Cells were harvested and lysed, and protein extracts were prepared. Viral protein expression was detected by immunoblotting using IE-, gB-, and pp28-specific antibodies. Equal protein loading was controlled for by including GAPDH.

hence slower-migrating form of IκBα (Fig. 6D). In addition, we found that UL138 expression not only upregulated TNFR1 surface expression in HeLa cells but also in THP-1 cells, i.e., in a cell line relevant for a simple model of latent HCMV infection (Fig. 6E). These data strongly suggest that the UL138 gene product is responsible for maintaining TNF-α responsiveness in HCMV-infected cells by securing TNFR1 surface expression.

To further test this hypothesis in a more physiological setting, we turned back to primary fibroblasts and asked whether exogenous expression of UL138 could rescue the TNF-α responsiveness of the ToledoΔUL133-138 mutant during infection. As shown in Fig. 7A, lentiviral infection worked well in primary fibroblasts and, as in HeLa cells, UL138 also upregulated TNFR1 on the surface of these cells. As seen before, infection of fibroblasts with ToledoΔUL133-138 efficiently downregulated TNFR1 surface expression (Fig. 7B, graphs I and II). Whereas neither UL133, UL135, nor UL136 could rescue TNFR1 surface expression, UL138 was clearly able to do so (graph VI). The functional significance of this observation is shown in Fig. 7C, as UL138 but not UL133, UL135, or UL136 could rescue TNF-α-induced NF-κB binding activity in ToledoΔUL133-138-infected fibroblasts. Of note, UL138 does

not require an additional gene product from the UL133-138 locus to exert this function. In addition, UL138 also affects the NF-κB pathway upstream of the DNA binding level, as shown by its destabilization of IκBα (Fig. 7D). This is consistent with the view that UL138 functions through upregulation of TNFR1 surface expression.

Given the above results, we finally wanted to address the question as to whether UL138 might modulate major IE gene expression in response to TNF-α. To this end, UL138 or control transduced HEL fibroblasts were transfected with a vector containing a subgenomic HCMV fragment encompassing just under 10 kb of the major IE gene locus. In this setting, UL138 but not UL133 could clearly stimulate expression from the major IE locus in response to TNF-α (Fig. 8). In view of the above results, the data are consistent with the notion that UL138 sensitizes the major IE gene locus to TNF-α-mediated activation by upregulating TNFR1 surface expression.

DISCUSSION

In our previous work we identified a mutant AD169 strain, termed AD169-varT, that unlike the commonly used and well-characterized strain AD169-varATCC had seemingly lost its ability to counteract TNF-α-induced activation of the NF-κB signaling pathway and, in contrast to AD169-varATCC, showed high, i.e., virtually unchanged, TNFR1 surface expression on infected cells (28). Here we have shown that, rather unexpectedly, AD169-varT contains additional genetic information and, although it must be considered a high-passage laboratory strain, AD169-varT harbors the ULb' region, which is a hallmark of low-passage strains and clinical isolates. We further showed that deletion of ULb' genes UL133 to UL138 minimizes surface expression of TNFR1 on infected cells and their responsiveness to TNF-α, as demonstrated by inhibition of NF-κB signaling. Consistent with this, isolated expression of UL138, but not UL133, UL134, UL135, or UL136, is able to upregulate TNFR1 on the surface of noninfected cells and, furthermore, UL138 expression functionally rescues both TNFR1 surface expression and NF-κB activation of cells infected with the ΔUL133-138 deletion mutant of HCMV. Thus, rather than AD169-varT, AD169-varATCC turns out to be the loss-of-function variant, and AD169-varT has retained the ability to keep TNFR1 surface expression high and, thereby, infected cells sensitive to TNF-α.

The denomination of AD169-varT reflects that this viral strain was originally identified because of its functional characteristics, namely, the inability to downregulate both TNFR1 surface expression and TNF-α-induced NF-κB activation. From these findings came a structural characterization that led to deciphering its relatedness to AD169 (28). Gene expression analysis has now revealed the presence of the ULb' region within AD169-varT (Fig. 1), and DNA sequencing of a central fragment of the ULb' region of AD169-varT further demonstrated that it was perfectly identical to a recently identified sequence from the ULb' region of AD169-varUC. Both AD169-varT and AD169-varUC contain within their ULb' region a unique 3.2-kb internal deletion (Fig. 1) (5). This characteristic feature strongly suggests that AD169-varT and AD169-varUC present the same AD169 variant. However, we can obviously not exclude variations between these two viruses
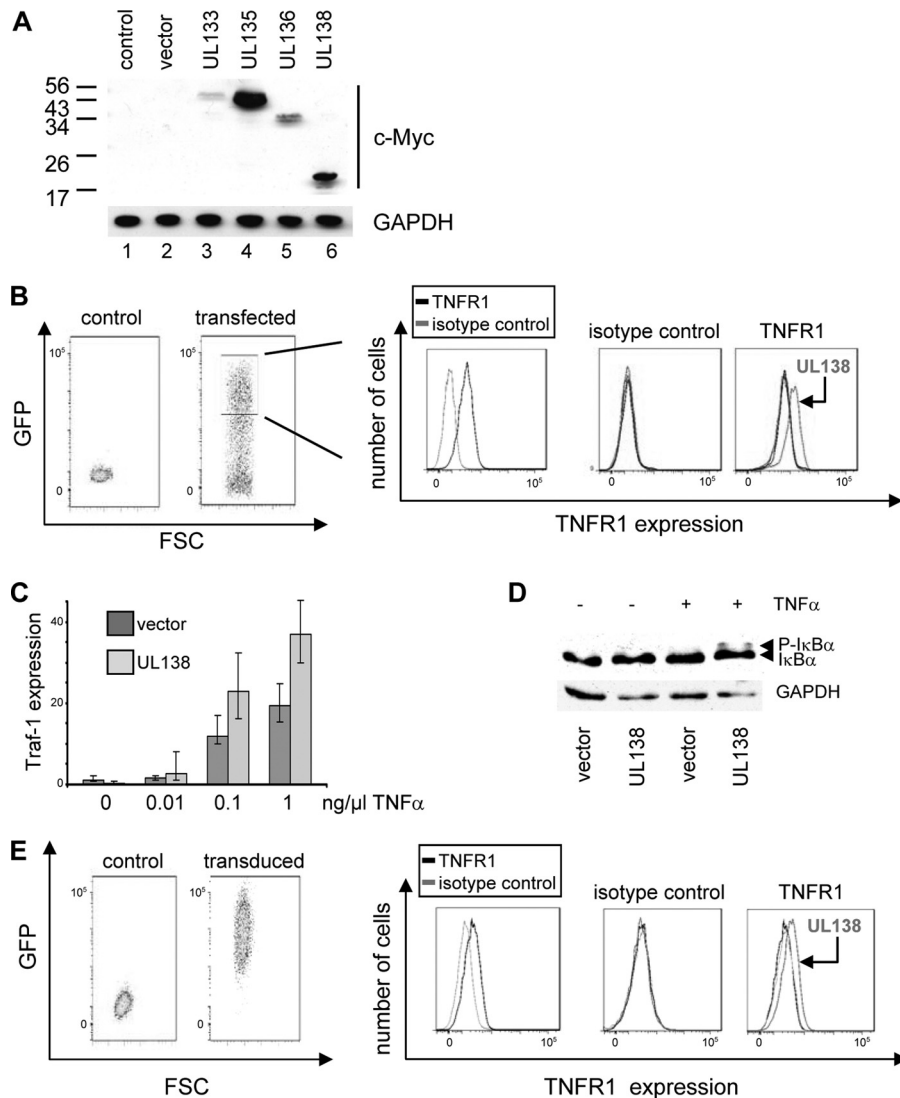
FIG. 6. UL138 upregulates TNFR1 surface expression in HeLa and THP-1 cells and potentiates TNF-α-induced NF-κB signaling. HeLa cells were transfected with lentiviral vectors expressing either the UL133, UL135, UL136, or UL138 gene in frame with a c-Myc epitope tag and, in addition, GFP. (A) Viral protein expression was detected by immunoblotting using a c-Myc-specific antibody. Equal protein loading was controlled by including GAPDH. (B) High-GFP-expressing HeLa cells were gated for each of the UL133-UL138-transfected populations as shown (boxed), and gated cells were analyzed for TNFR1 surface expression as described for Fig. 3D. Expression analyses are shown as overlay histograms. (C) Mock- and UL138-transfected HeLa cells were puromycin selected and stimulated with TNF-α for 2 h, employing the indicated concentrations. RNA was prepared, and Traf-1 expression was analyzed by real time-PCR with normalization to GAPDH expression. (D) Transfected cells as described for panel C were treated with the proteasome inhibitor ALLN for 1 h, and phosphorylation of IκBα was detected by immunoblotting in the absence or presence of 0.01 ng/ml TNF-α (10 min). Equal protein loading was controlled for by including GAPDH. (E) TH-P1 cells were either left untransduced or were transduced with an empty lentivirus or a UL138-expressing lentivirus and puromycin selected as indicated by GFP detection. TNR1 surface expression was analyzed in all three populations, and TNFR1 surface expression is shown in the overlay histograms.

outside the sequenced fragment. Since no functional studies have been performed with AD169-varUC yet, this work and our previously published data (28) present the first functional characterization of a ULb′-containing variant of AD169.

The existence of a ULb′-containing variant of AD169 is reminiscent of the situation found in strain Towne. ATCC Towne (VR-977) has been demonstrated to contain a mixture of two variants, i.e., Towne$_{short}$, which lacks ULb′ sequence, and Towne$_{long}$, which includes this genomic fragment (11, 12, 20, 29). Thus, in principle, AD169-varT and AD160-varATCC somehow reflect the situation found in Towne. However, anal-

ysis of ATCC AD169 showed no contamination with the ULb′-containing variant varT (C. Montag and C. Hagemeier, unpublished observation).

We unknowingly received the variant AD169-varT when we requested an AD169 virus from B. Plachter (University of Mainz, Mainz, Germany). It appears that the virus received by us at the time goes back to an aliquot of an early AD169 preparation that was given to the Institute of Virology in Erlangen (B. Plachter, personal communication). Thus, our attempt to backtrack AD169-varT is in agreement with the conclusion drawn by Bradley et al., that AD169-varUC is likely to
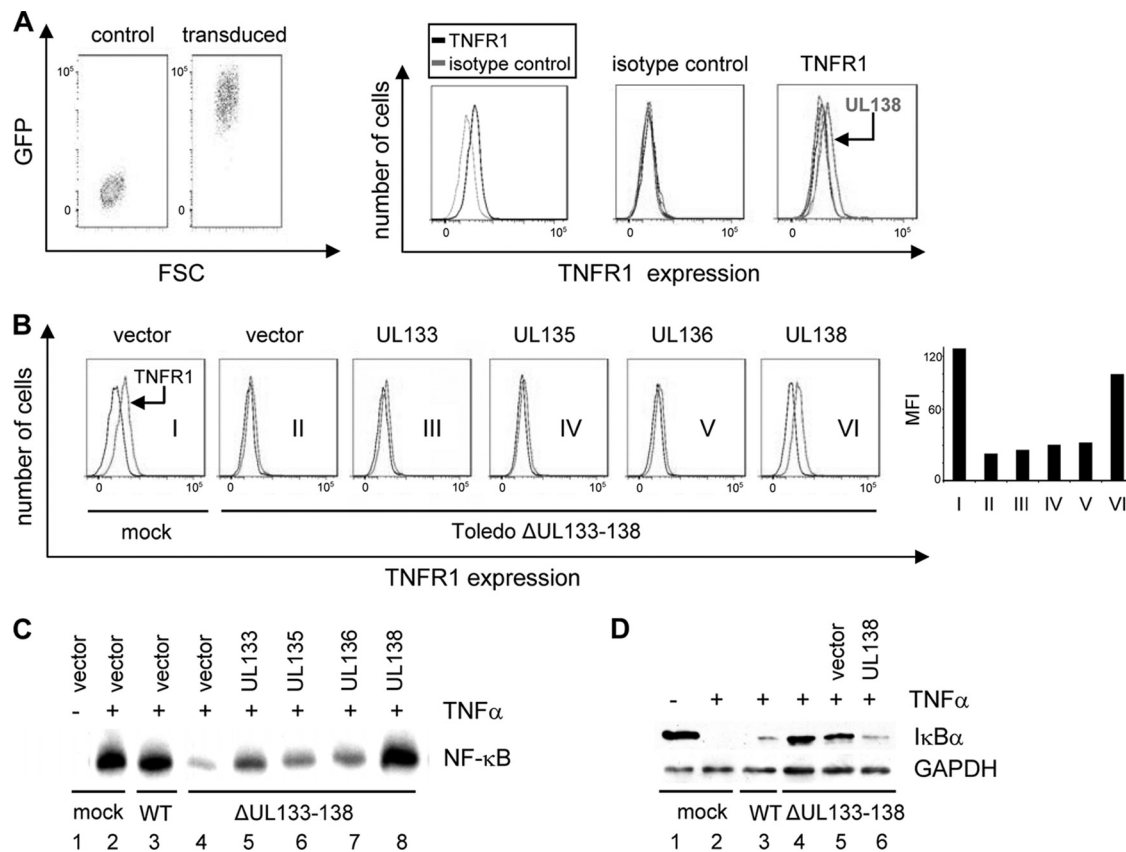
FIG. 7. UL138 rescues TNFR1 surface expression and TNF-α-induced NF-κB activation in ToledoΔUL133-138-infected cells. (A) Primary fibroblasts were transduced with lentiviruses expressing UL133, UL135, UL136, or UL138 and puromycin selected to yield a population of greater than 99% transduced cells as indicated by GFP detection. TNR1 surface expression was analyzed in each of the GFP-positive populations expressing one of the viral UL133 to UL138 genes as described for Fig. 6. (B) Primary fibroblasts transduced with lentiviral vectors for UL133 to UL138 were either mock infected or infected with the ToledoΔUL133-138 mutant virus as indicated. At 72 h post-HCMV infection, surface expression of TNFR1 was analyzed (graphs I to VI). The bar chart shows a quantitative analysis (mean fluorescence intensity minus that of an isotype control) of the depicted histograms generated by using the FlowJo analysis software (Becton Dickinson). (C) Primary fibroblasts transduced with either control lentivirus or the indicated UL133- to UL138-expressing lentiviral constructs were superinfected with Toledo wild type (WT; lane 3), ToledoΔUL133-138 (lanes 4 to 8), or mock infected (lanes 1 and 2). After TNF-α stimulation for 10 min, cells were harvested, nuclear extracts were prepared, and NF-κB DNA binding was detected by EMSA. (D) Control cells (lanes 1 and 2), Toledo WT-infected cells (lane 3), and ToldeoΔUL133-138-infected cells (lanes 3 to 6) either transduced with a lentiviral vector (lane 5) or a UL138-expressing lentivirus (lane 6) were stimualted with TNF-α for 10 min (lanes 2 to 6). The abundance of IκBα was detected by immunoblotting. Equal protein loading was controlled for by including GAPDH.

have evolved from an original ancestor before the loss of the ULb′ region from AD169 (5). More importantly, this raises the question of strain (variant) fidelity. AD169 is a widely used strain that has been employed for many important milestone publications in the field. It appears likely that ULb′-positive and -negative AD169 variants have been employed for these studies, and this might help to explain the difficulties in the reproducibility of certain experimental results despite the use of the seemingly same viral strain, namely, AD169.

Variants can be instrumental for identification of viral functions that would otherwise be masked, and this is also the case for the findings presented here. TNFR1 surface expression can clearly be detected on noninfected primary fibroblasts, and AD169-varATCC, i.e., a ULb′-negative strain, strongly downregulates this expression around early times of infection (2, 28) (Fig. 3, 4, and 7). However, in AD169-varT, i.e., a ULb′-positive strain, TNFR1 surface expression on infected cells can be well detected albeit to a slightly reduced level than in non-

infected control cells (Fig. 3). Thus, these results unfold a more complex regulation of TNFR1 surface expression and TNF-α sensitivity of HCMV-infected cells. Why HCMV contains a positive and negative regulator for TNF-α responsiveness is currently unclear. However, the ULb′ region encodes gene products that control the host's immune response, cell tropism, and latency. Therefore, it needs to be considered that TNF-α responsiveness may play a role in one or both of these viral functions, and the identification of UL138 as a regulator of TNFR1 surface expression further supports this view (see below).

In this report, we have not followed up on the HCMV inhibitor of TNFR1 surface expression. This so-far-unidentified factor acts at early times of infection and independently of TNF-α. Therefore, the observed downregulation cannot be explained by receptor internalization after ligand binding or by viral attachment to the cell surface *per se*. The latter has been shown for cytokine receptors like CCR1, CCR2, CCR5, and
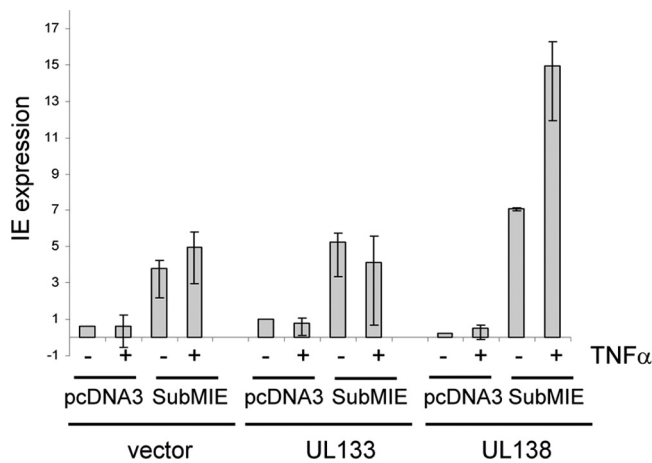
FIG. 8. UL138 enhances TNF-α-induced IE gene expression. HEL fibroblasts transduced with either UL133- or UL138-expressing lentiviruses were serum starved for 72 h and nucleotransfected with either a pcDNA3 control vector (pcDNA3) or a sub-MIE construct containing a subgenomic fragment of HCMV from nucleotide −1338 to +8409 relative to the transcription start site of the MIE gene. Electroporated cells were then cultured in the absence or presence of TNF-α (30 ng/ml) for 4 h in the absence of serum. After cell harvest, RNAs were prepared and IE expression analyzed by real time-PCR with normalization to L32 expression.

CXCR4, and the viral UL128-UL131A subcomplex appears to play an important role in that at times of viral entry (15, 45). However, the time window of this receptor downregulation and the fact that the UL128-UL131 complex is rendered nonfunctional bot in AD169 and Toledo make it unlikely that these factors play a role in the observed inhibition of TNFR1 surface expression.

In contrast, here we have identified the ULb′-encoded UL138 gene product as an inducer of TNFR1 surface expression. Clearly, when UL138 is expressed independently of a viral infection, it is sufficient to increase TNFR1 surface expression. In lytically infected cells, this is reflected by a lack of TNFR1 downregulation, paying tribute to the additional viral activity that downregulates TNFR1 surface expression, which is the dominant outcome for cells infected with viruses lacking the ULb′ region. UL138 is expressed as part of a polycistronic transcript that, in addition to UL138, also includes open reading frames for UL133, UL134, UL135, and UL136 (17), and when this transcriptional unit is deleted from the viral background, TNFR1 surface expression and TNF-α responsiveness are severely, albeit not completely, diminished (Fig. 4). Importantly, isolated expression of UL138 can rescue both viral activities, demonstrating that UL138 is the single most important factor in the upregulation of TNFR1 surface expression. However, this does not exclude that additional viral factors contribute to TNFR1 upregulation. These other factors might be encoded by UL133 to UL136 and, as supported by the finding in Fig. 4B, one or more ULb′-encoded factors outside the UL133-UL138 gene locus appear to contribute an independent NF-κB-regulating activity. Currently, it is unclear which viral factors might cooperate with this UL138 function. UL144, a ULb′-located viral member of the TNFR superfamily that has previously been shown to regulate NF-κB activity (33), does not affect TNF-α responsiveness when specifically de-

leted from strain Toledo (Fig. 4 and data not shown). Also, it does not function by modifying TNFR1 surface expression, but rather by a signaling complex involving TRAF6 and TRIM23 (32). In addition, most of the UL144 gene is lost from AD169-varT due to its internal deletion of the 3.2-kb fragment (Fig. 1) (5).

Baillie et al. were the first to show that TNFR1 surface expression is reduced when cells are infected with HCMV and, of note, strain AD169 was employed in their studies (2). They demonstrated that TNFR1 steady-state protein levels showed little difference between AD169-infected and noninfected cells. Rather, the known Golgi apparatus-to-cell surface ratio of TNFR1 (23) was shifted in favor of the Golgi apparatus-localized receptor, suggesting that during TNFR1 trafficking in AD169-infected cells the receptor becomes retained in the Golgi apparatus. Interestingly, UL138 has also been reported to localize to the Golgi apparatus (31). These observations are consistent with the functional interaction between UL138 and TNFR1 shown here and further suggest a possible mechanistic link in that UL138 might counteract TNFR1 retention in the Golgi apparatus, thereby increasing the surface availability of TNFR1.

As alluded to in the introduction, several viruses target TNFR1 function. However, under these circumstances TNFR1 becomes inhibited and, mechanistically, viruses have evolved different approaches to reach this goal, including downregulation of surface TNFR1. Given the antiviral properties of TNF-α, this underscores the significance of restraining TNF-α signaling for a number of different viruses, including some herpesviruses (see above). Why then should HCMV increase TNFR1 surface availability? First, it needs to be remembered that HCMV also contains an activity that downregulates TNFR1 (function) (Fig. 2) (2, 28), and the TNFR1-upregulating function identified here is an additional independent activity of HCMV. Thus, TNFR1 agonistic and antagonistic functions of HCMV are likely to be differentially regulated and to serve distinct biological functions during the course of infection. Given the very limited number of genes expressed during latency, downregulation of TNFR1 by HCMV is likely to be more relevant during lytic infection. Second, TNFR1 availability is apparently not required for lytic viral infection, and this points to other physiological conditions under which UL138-mediated upregulation of TNFR1 might be more relevant. Of particular interest in this respect is that the UL138 expression pattern and its localization to the Golgi network has recently been linked to the latent state of HCMV infection (16, 31). This provokes the hypothesis that UL138 may foster TNFR1 surface expression particularly on latently infected cells, thereby promoting a state of increased sensitivity to TNF-α (Fig. 9). Indeed, in monocytes, which are a site for HCMV latency in vivo (39), TNF-α has been shown to promote an HCMV permissive state by triggering their differentiation toward postmitotic macrophages (41). Besides promoting cellular susceptibility, TNF-α has also been reported to more directly stimulate the activity of the MIE promoter/enhancer in vitro (44). Given the potent NF-κB-inducing activity of TNF-α, it is interesting that the well-studied NF-κB binding sites within the MIE promoter/enhancer are dispensable for the HCMV lytic cycle in dividing cells (4), whereas in nondividing quiescent cells they are critical for IE expression and HCMV
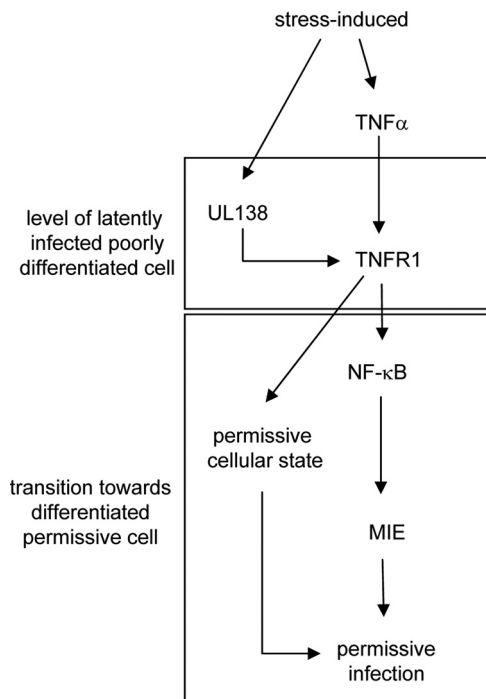
FIG. 9. Hypothetical schematic concerning the UL138-TNFR1 interplay. For this hypothetical setting, a latently infected, poorly differentiated cell was considered. However, it is neither suggested that the UL138-TNFR1 interaction is sufficient to drive reactivation, nor has it been shown that this functional interaction exists in latently infected cells. Rather, this model serves as a rationale to envisage a biological function of this interaction with respect to published evidence. Since during latency only a very limited number of viral genes are expressed, those viral activities downregulating TNFR1 expression during lytic infection are likely to be absent at this stage and, therefore, were omitted from this model. Under stress conditions, UL138 becomes upregulated (17) and induces TNFR1 surface expression that allows TNF-α-mediated signaling (present study). TNF-α signaling is conducive to the development of an HCMV-permissive state in differentiating cells (41) and promotes, via NF-κB, viral major IE gene expression (6). Together, this contributes to a cellular and viral state that could foster reactivation.

replication (6). Of note, we have shown that UL138 hypersensitizes the major IE gene to TNF-α (Fig. 8). Thus, by upregulating TNFR1 surface availability, UL138 may promote a window of opportunity for reactivation from HCMV latency by sensitizing cells to TNF-α, which in turn drives cellular processes (differentiation) and viral processes (major IE activation) that are important to HCMV reactivation from latency.

The UL138 gene product has previously been suggested to be required for the induction of latency (16). How does that relate to the data presented here? First, the effect observed in the study by Goodrum et al. might have been caused by a lack of reactivation rather than or in addition to a lack of induction of latency. Second, gene expression from the UL138 locus appears to be complex (17), and different forms of UL138 may well be responsible for different activities. Third, UL138 might exert distinct functions in different cell types. Fourth, it appears a rather attractive consideration that UL138 can indeed promote two functions, i.e., it is necessary for the induction of

a latent state and at the same time sets up a sensing mechanism in latently infected cells that fosters viral escape from latency.

REFERENCES

1. **Atalay, R., et al.** 2002. Identification and expression of human cytomegalovirus transcription units coding for two distinct Fcγ receptor homologs. J. Virol. **76:**8596–8608.
2. **Baillie, J., D. A. Sahlender, and J. H. Sinclair.** 2003. Human cytomegalovirus infection inhibits tumor necrosis factor alpha (TNF-alpha) signaling by targeting the 55-kilodalton TNF-alpha receptor. J. Virol. **77:**7007–7016.
2a.**Bartee, E., M. R. Mohamed, and G. McFadden.** 2008. Tumor necrosis factor and interferon: cytokines in harmony. Curr. Opin. Microbiol. **11:**378–383.
3. **Bego, M., J. Maciejewski, S. Khaiboullina, G. Pari, and S. St Jeor.** 2005. Characterization of an antisense transcript spanning the UL81-82 locus of human cytomegalovirus. J. Virol. **79:**11022–11034.
4. **Benedict, C. A., et al.** 2004. Neutrality of the canonical NF-κB-dependent pathway for human and murine cytomegalovirus transcription and replication in vitro. J. Virol. **78:**741–750.
5. **Bradley, A. J., et al.** 2009. High-throughput sequence analysis of variants of human cytomegalovirus strains Towne and AD169. J. Gen. Virol. **90:**2375–2380.
6. **Caposio, P., A. Luganini, G. Hahn, S. Landolfo, and G. Gribaudo.** 2007. Activation of the virus-induced IKK/NF-κB signalling axis is critical for the replication of human cytomegalovirus in quiescent cells. Cell. Microbiol. **9:**2040–2054.
7. **Cha, T. A., et al.** 1996. Human cytomegalovirus clinical isolates carry at least 19 genes not found in laboratory strains. J. Virol. **70:**78–83.
8. **Chee, M. S., et al.** 1990. Analysis of the protein-coding content of the sequence of human cytomegalovirus strain AD169. Curr. Top. Microbiol. Immunol. **154:**125–169.
9. **Chuang, H. C., et al.** 2007. Epstein-Barr virus (EBV) latent membrane protein-1 down-regulates tumor necrosis factor-alpha (TNF-alpha) receptor-1 and confers resistance to TNF-alpha-induced apoptosis in T cells: implication for the progression to T-cell lymphoma in EBV-associated hemophagocytic syndrome. Am. J. Pathol. **170:**1607–1617.
10. **Dargan, D. J., et al.** 2010. Sequential mutations associated with adaptation of human cytomegalovirus to growth in cell culture. J. Gen. Virol. **91:**1535–1546.
11. **Dolan, A., et al.** 2004. Genetic content of wild-type human cytomegalovirus. J. Gen. Virol. **85:**1301–1312.
12. **Dunn, W., et al.** 2003. Functional profiling of a human cytomegalovirus genome. Proc. Natl. Acad. Sci. U. S. A. **100:**14223–14228.
13. **Fessler, S. P., Y. R. Chin, and M. S. Horwitz.** 2004. Inhibition of tumor necrosis factor (TNF) signal transduction by the adenovirus group C RID complex involves downregulation of surface levels of TNF receptor 1. J. Virol. **78:**13113–13121.
14. **Filippova, M., H. Song, J. L. Connolly, T. S. Dermody, and P. J. Duerksen-Hughes.** 2002. The human papillomavirus 16 E6 protein binds to tumor necrosis factor (TNF) R1 and protects cells from TNF-induced apoptosis. J. Biol. Chem. **277:**21730–21739.
15. **Frascaroli, G., et al.** 2009. Human cytomegalovirus paralyzes macrophage motility through down-regulation of chemokine receptors, reorganization of the cytoskeleton, and release of macrophage migration inhibitory factor. J. Immunol. **182:**477–488.
16. **Goodrum, F., M. Reeves, J. Sinclair, K. High, and T. Shenk.** 2007. Human cytomegalovirus sequences expressed in latently infected individuals promote a latent infection in vitro. Blood **110:**937–945.
17. **Grainger, L., et al.** 2010. Stress-inducible alternative translation initiation of human cytomegalovirus latency protein pUL138. J. Virol. **84:**9472–9486.
18. **Greaves, R. F., and E. S. Mocarski.** 1998. Defective growth correlates with reduced accumulation of a viral DNA replication protein after low-multiplicity infection by a human cytomegalovirus ie1 mutant. J. Virol. **72:**366–379.
19. **Hahn, G., R. Jores, and E. S. Mocarski.** 1998. Cytomegalovirus remains latent in a common precursor of dendritic and myeloid cells. Proc. Natl. Acad. Sci. U. S. A. **95:**3937–3942.
20. **Hahn, G., D. Rose, M. Wagner, S. Rhiel, and M. A. McVoy.** 2003. Cloning of the genomes of human cytomegalovirus strains Toledo, Towne-varRIT3, and Towne long as BACs and site-directed mutagenesis using a PCR-based technique. Virology **307:**164–177.

20a. Herbein, G., and W. A. O'Brien. 2000. Tumor necrosis factor (TNF)-alpha and TNF receptors in viral pathogenesis. Proc. Soc. Exp. Biol. Med. 223: 241–257.

21. Jarvis, M. A., et al. 2006. Human cytomegalovirus attenuates interleukin-1β and tumor necrosis factor alpha proinflammatory signaling by inhibition of NF-κB activation. J. Virol. 80:5588–5598.

22. Jenkins, C., A. Abendroth, and B. Slobedman. 2004. A novel viral transcript with homology to human interleukin-10 is expressed during latent human cytomegalovirus infection. J. Virol. 78:1440–1447.

23. Jones, S. J., et al. 1999. TNF recruits TRADD to the plasma membrane but not the trans-Golgi network, the principal subcellular location of TNF-R1. J. Immunol. 162:1042–1048.

24. Kondo, K., H. Kaneshima, and E. S. Mocarski. 1994. Human cytomegalovirus latent infection of granulocyte-macrophage progenitors. Proc. Natl. Acad. Sci. U. S. A. 91:11879–11883.

24a. Landolfo, S., M. Gariglio, G. Gribaudo, and D. Lembo. 2003. The human cytomegalovirus. Pharmacol. Ther. 98:269–297.

25. Liang, L., and B. Roizman. 2006. Herpes simplex virus 1 precludes replenishment of the short-lived receptor of tumor necrosis factor alpha by virion host shutoff-dependent degradation of its mRNA. J. Virol. 80:7756–7759.

26. Minton, E. J., C. Tysoe, J. H. Sinclair, and J. G. Sissons. 1994. Human cytomegalovirus infection of the monocyte/macrophage lineage in bone marrow. J. Virol. 68:4017–4021.

27. Reference deleted.

28. Montag, C., J. Wagner, I. Gruska, and C. Hagemeier. 2006. Human cytomegalovirus blocks tumor necrosis factor alpha- and interleukin-1β-mediated NF-κB signaling. J. Virol. 80:11686–11698.

29. Murphy, E., et al. 2003. Coding potential of laboratory and clinical strains of human cytomegalovirus. Proc. Natl. Acad. Sci. U. S. A. 100:14976–14981.

30. Neznanov, N., et al. 2001. Poliovirus protein 3A inhibits tumor necrosis factor (TNF)-induced apoptosis by eliminating the TNF receptor from the cell surface. J. Virol. 75:10409–10420.

31. Petrucelli, A., M. Rak, L. Grainger, and F. Goodrum. 2009. Characterization of a novel Golgi apparatus-localized latency determinant encoded by human cytomegalovirus. J. Virol. 83:5615–5629.

32. Poole, E., et al. 2009. Identification of TRIM23 as a cofactor involved in the regulation of NF-κB by human cytomegalovirus. J. Virol. 83:3581–3590.

33. Poole, E., C. A. King, J. H. Sinclair, and A. Alcami. 2006. The UL144 gene product of human cytomegalovirus activates NFκB via a TRAF6-dependent mechanism. EMBO J. 25:4390–4399.

34. Prichard, M. N., M. E. Penfold, G. M. Duke, R. R. Spaete, and G. W. Kemble. 2001. A review of genetic differences between limited and extensively passaged human cytomegalovirus strains. Rev. Med. Virol. 11:191–200.

35. Reeves, M. B., P. J. Lehner, J. G. Sissons, and J. H. Sinclair. 2005. An in vitro model for the regulation of human cytomegalovirus latency and reactivation in dendritic cells by chromatin remodelling. J. Gen. Virol. 86:2949–2954.

36. Revello, M. G., and G. Gerna. 2010. Human cytomegalovirus tropism for endothelial/epithelial cells: scientific background and clinical implications. Rev. Med. Virol. 20:136–155.

37. Saederup, N., and E. S. Mocarski, Jr. 2002. Fatal attraction: cytomegalovirus-encoded chemokine homologs. Curr. Top. Microbiol. Immunol. 269: 235–256.

38. Sedger, L. M., et al. 2006. Poxvirus tumor necrosis factor receptor (TNFR)-like T2 proteins contain a conserved preligand assembly domain that inhibits cellular TNFR1-induced cell death. J. Virol. 80:9300–9309.

39. Sinclair, J., and P. Sissons. 2006. Latency and reactivation of human cytomegalovirus. J. Gen. Virol. 87:1763–1779.

40. Sinzger, C., M. Digel, and G. Jahn. 2008. Cytomegalovirus cell tropism. Curr. Top. Microbiol. Immunol. 325:63–83.

41. Soderberg-Naucler, C., K. N. Fish, and J. A. Nelson. 1997. Interferon-gamma and tumor necrosis factor-alpha specifically induce formation of cytomegalovirus-permissive monocyte-derived macrophages that are refractory to the antiviral activity of these cytokines. J. Clin. Invest. 100:3154–3163.

42. Soderberg-Naucler, C., K. N. Fish, and J. A. Nelson. 1997. Reactivation of latent human cytomegalovirus by allogeneic stimulation of blood cells from healthy donors. Cell 91:119–126.

43. Stanton, R. J., et al. 2010. Reconstruction of the complete human cytomegalovirus genome in a BAC reveals RL13 to be a potent inhibitor of replication. J. Clin. Invest. 120:3191–3208.

44. Stein, J., H. D. Volk, C. Liebenthal, D. H. Kruger, and S. Prosch. 1993. Tumour necrosis factor alpha stimulates the activity of the human cytomegalovirus major immediate early enhancer/promoter in immature monocytic cells. J. Gen. Virol. 74:2333–2338.

45. Straschewski, S., et al. 2011. Protein pUL128 of human cytomegalovirus is necessary for monocyte infection and block of migration. J. Virol. 85:5150–5158.

46. Taylor-Wiedeman, J., G. P. Hayhurst, J. G. Sissons, and J. H. Sinclair. 1993. Polymorphonuclear cells are not sites of persistence of human cytomegalovirus in healthy individuals. J. Gen. Virol. 74:265–268.

47. Taylor-Wiedeman, J., J. G. Sissons, L. K. Borysiewicz, and J. H. Sinclair. 1991. Monocytes are a major site of persistence of human cytomegalovirus in peripheral blood mononuclear cells. J. Gen. Virol. 72:2059–2064.

48. Wang, W., et al. 2005. Human cytomegalovirus genes in the 15-kilobase region are required for viral replication in implanted human tissues in SCID mice. J. Virol. 79:2115–2123.

49. Wilkinson, G. W., et al. 2008. Modulation of natural killer cells by human cytomegalovirus. J. Clin. Virol. 41:206–212.

50. Yang, S., et al. 2006. Using DNA microarray to study human cytomegalovirus gene expression. J. Virol. Methods 131:202–208.

51. Zydek, M., C. Hagemeier, and L. Wiebusch. 2010. Cyclin-dependent kinase activity controls the onset of the HCMV lytic cycle. PLoS Pathog. 6:31001096.

51a. Zydek, M., et al. General blockade of HCMV immediate early mRNA expression in SIG2 by a nuclear, Daxx- and PML-independent mechanism. J. Gen. Virol., in press.